

## A Novel Graphene-Supported Palladium Catalyst for Suzuki–Miyaura Coupling of Less Reactive Heteroaryl Halides in Water

Abu Taher,<sup>†</sup> Dong-Jin Lee,<sup>†</sup> Ik-Mo Lee,<sup>†,\*</sup> Md. Lutfor Rahman,<sup>‡</sup> and Md. Shaheen Sarker<sup>‡,\*</sup>

<sup>†</sup>Department of Chemistry, Inha University, Incheon 402-751, South Korea. \*E-mail: imlee@inha.ac.kr

<sup>‡</sup>Faculty of Industrial Sciences and Technology, University Malaysia Pahang, 26300 Gambang, Kuantan, Pahang, Malaysia. \*E-mail: shaheen@ump.edu.my

Received June 8, 2016, Accepted July 20, 2016, Published online August 29, 2016

An efficient reduced graphene oxide-supported heterogenized palladium complex with pyrene-tagged ketoiminato ligand has been developed and used for cross-coupling of less reactive heteroaryl halides in water. Desirable catalytic activity was observed with high (up to 98%) conversion of the less reactive reactants under relatively mild conditions. The efficiency and green nature of the catalyst were confirmed without significant loss of activity.

**Keywords:** Graphene oxide, Heterogeneous catalyst, Palladium, Cross-coupling, Heteroaryl halides

### Introduction

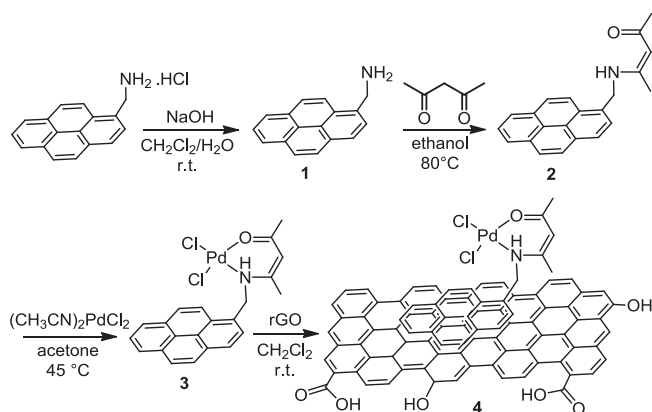
Heterobiaryl compounds are a very common structural motif in various natural products, pharmaceuticals, and biologically active organic molecules.<sup>1</sup> The palladium (Pd)-catalyzed Suzuki–Miyaura coupling (SMC) reaction is one of the most characteristic and frequently used methods to construct such carbon–carbon bonds in organic synthesis,<sup>2</sup> as it facilitates the coupling of heteroaryl halides with boronic acids. In recent years, SMC reactions have received much attention for the synthesis of heteroatom-containing biaryl compounds with great industrial potential.<sup>3</sup> Even though a large number of reports have been published in this field of research, most heterocyclic coupling partners have not been widely used<sup>4</sup> and only limited progress has been made in heterobiaryl production. This may be due to the fact that coupling reactions with heteroaryl substrates have proven more challenging than the analogous couplings of simpler substrates. Thus, more efficient catalytic methods for the corresponding coupling products are required.<sup>5</sup> Even though satisfactory results have been obtained in limited cases, long reaction time at relatively high temperature and pressure was usually required.<sup>3</sup>

On the other hand, the incorporation of a homogeneous catalyst onto a support is one of the most challenging work in the field of catalysis, because this allows easier reprocessing of the used catalyst.<sup>6</sup> In addition, recycling of homogeneous metal catalysts is considered one of the important objectives in the field of green chemistry.<sup>7</sup> One such an environmentally benign process involves the development of solid-supported catalysts exhibiting high catalytic efficiency even in an aqueous medium.<sup>8</sup> Thus, efforts have been made to immobilize homogeneous catalysts on various support materials, such as nanoparticles,<sup>9</sup> inorganic solids,<sup>10</sup> polymers,<sup>11</sup> dendrimers,<sup>12</sup> and perfluorinated tags.<sup>13</sup> Graphene surfaces have recently gained much

attention due to their convenient molecular attachment in organic synthesis.<sup>14</sup> The widely used covalent immobilization strategies often require nontrivial pretreatment of the solid surface. However, noncovalent methods exploiting strong  $\pi$  interactions between poly-aromatic hydrocarbons and nano-graphitized surfaces offer a convenient and practical approach for the immobilization. Therefore, noncovalent methods<sup>6</sup> have attracted great interest in the field of catalysis. Because of the inherent nature of the pyrene moiety to afford noncovalent interactions with nano-graphitic surfaces,<sup>15</sup> complexes with a pyrene tag have been introduced on graphitized surfaces<sup>16</sup> and have also been used in catalysis, proving interesting recyclability properties.<sup>17</sup> Despite these impressive recent improvements, the catalytic protocol still suffers from some disadvantages, such as metal leaching and low reactivity for several important substrate classes. Therefore, the development of reusable catalysts for the SMC reaction under mild conditions is highly desirable from the view points of both green chemistry and current organic synthesis. Here we report a highly efficient and reusable rGO-supported Pd complex (**4**) for the cross-coupling of less reactive and sterically hindered heteroaryl halides in water under mild reaction conditions (Scheme 1).

### Experimental

**General Information.** All reagents were purchased from commercial sources and used without any prior purification, unless otherwise stated. <sup>1</sup>H and <sup>13</sup>C NMR spectra were recorded at either 300 or 400 MHz. Chemical shifts were measured in parts per million ( $\delta$  ppm) referenced to the solvent peak or 0.0 ppm for tetramethylsilane peak. The FT-IR spectra were obtained on a Nicolet iS10 FT-IR spectrometer. All products were isolated by chromatography using a silica gel (0.035–0.070 mm) column, unless otherwise noted. X-ray powder diffraction (XRD) patterns were



**Scheme 1.** Synthesis of reduced graphene oxide-supported catalyst **4**.

recorded on a Rigaku diffractometer using Cu K $\alpha$  radiation ( $\lambda = 1.54 \text{ \AA}$ ). X-ray photoelectron spectroscopy (XPS) measurements were carried out on a K-Alpha instrument (Thermo Scientific). For transmission electron microscopy (TEM) measurements, a drop of the sample suspension was placed on Formvar and carbon-coated positive-glow-discharge-treated copper grid and subsequently blotted dry by a filter paper. The prepared samples were examined in a JEM-2100 F field-emission transmission electron microscope (FE-TEM) with energy dispersive spectroscopy (EDS) and the images were recorded using a charge-coupled device camera. Scanning electron microscopy (SEM) images and EDS elemental mapping were observed with an SU8010 microscope (Hitachi, Japan). Thermogravimetric analysis (TGA) was carried out on a Scinco S-1000 system under a N<sub>2</sub> gas flow. The Raman spectra were measured using an excitation wavelength of 457.9 nm provided by a Spectra-Physics model 2025 argon ion laser. Elemental analysis was carried out using a Flash EA1112 analyzer (Thermo Electron Corporation). Gas chromatography (GC) or GC–mass spectrometry (GC–MS) was performed on an Agilent 6890N GC coupled to an Agilent 5975 Network mass-selective detector. The Pd content was measured using inductively coupled plasma-atomic emission spectroscopy (ICP-AES) by an OPTIMA 4300 DV instrument (Perkin-Elmer). UV–vis spectra (diffuse reflectance mode) were recorded on a UV–vis spectrophotometer (Varian, Australia). The spectra were recorded in the range 200–800 nm using boric acid as the standard of reflectance.

**Synthesis of (Pyren-1-yl)methanamine (1).** A solution of NaOH (0.054 g, 1.34 mmol) in water (12 mL) was added dropwise to a stirring solution of 1-pyrenemethylamine hydrochloride (0.30 g, 1.12 mmol) in methylene chloride (MC) (12 mL). The resulting solution was gently stirred at room temperature (RT) for 0.5 h and, at the end of reaction, the color changed from yellow to white. The reaction mixture was diluted with MC and separated. The organic layer was dried over magnesium sulfate (MgSO<sub>4</sub>) and evaporated under reduced pressure. The crude reaction product was

purified by column chromatography using MeOH as an eluent to afford (pyren-1-yl)methanamine **1** in 90% (0.24 g) yield. <sup>1</sup>H NMR (400 MHz, CDCl<sub>3</sub>)  $\delta$  8.31–7.97 (m, 9H, arom); 4.56 (d, 2H,  $J = 1.2$  Hz); 1.66 (s, 2H); <sup>13</sup>C NMR (100 MHz, CDCl<sub>3</sub>)  $\delta$  136.74–122.67 (16C, arom), 44.33 (s, 1C,  $\alpha$ ); IR (cm<sup>-1</sup>): 3364 (N–H stretch), 3038 (C–H, arom), 1570 (C=C, arom), 1183 (C–N, stretch), 881, 838 and 709 (C–H, bend); Anal. Calcd. for C<sub>17</sub>H<sub>13</sub>N (231.29): C, 88.28; H, 5.67; N, 6.06. Found: C, 88.02; H, 5.83; N, 5.91%.

**Synthesis of 4-((Pyren-1-yl)methylamino)pent-3-en-2-one (2).** A solution of pentane-2,4-dione (0.171 g, 1.72 mmol) in absolute ethanol (6 mL) was added dropwise with continuous stirring to a solution of (pyren-1-yl)methanamine **1** (0.36 g, 1.56 mmol) in ethanol (10 mL). The resulting solution was mildly refluxed with stirring for 12 h. The color changed from pale green to bright orange. The reaction mixture was then allowed to cool at RT and concentrated under reduced pressure. After purification of the crude product using silica gel column chromatography (EtOAc/hexane, 1:1), **2** was obtained as a white solid in 68% (0.329 g) yield. <sup>1</sup>H NMR (400 MHz, CDCl<sub>3</sub>):  $\delta$  11.39 (s, 1H, NH); 8.18–7.89 (m, 9H, C–H, Ar); 5.11 (d, 2H,  $J = 6.4$  Hz); 5.09 (s, 1H, CH); 2.06 (s, 3H, CH<sub>3</sub>); 1.99 (s, 3H, CH<sub>3</sub>) ppm; <sup>13</sup>C NMR (100 MHz, CDCl<sub>3</sub>):  $\delta$  195.45, 163.06, 131.21–121.71 (16C, Ar), 96.14, 44.81, 28.88, 18.96 ppm; IR (cm<sup>-1</sup>): 3283 (N–H stretch, amine), 3037 (C–H, Ar), 2919 (C–H, Al), 1662 (C=O), 1581 (C=C, Ar), 1190 (C–N stretch), 837, 748 and 705 (C–H “oop,” Ar); Anal. Calcd. for C<sub>22</sub>H<sub>19</sub>NO (313.39): C, 84.31; H, 6.11; N, 4.47. Found: C, 84.36; H, 6.34; N, 5.01%.

**Synthesis of Pyrene-tagged Pd complex (3).** A solution of (CH<sub>3</sub>CN)<sub>2</sub>PdCl<sub>2</sub> (0.27 g, 1.05 mmol) in acetone (9 mL) was added to a stirred solution of 4-((pyren-1-yl)methylamino)pent-3-en-2-one **2** (0.33 g, 1.05 mmol, acetone, 7 mL). The resulting solution was gently stirred at 45°C for 2 h during which time, pale orange crystals precipitated out. The reaction flux was then removed from the heating bath and allowed to cool at room temperature. The products were separated by filtration and washed repeatedly with acetone to give the corresponding pyrene-tagged Pd-complex **3** in 80% (0.41 g) yield. <sup>1</sup>H NMR (400 MHz, DMSO-*d*<sub>6</sub>):  $\delta$  11.07 (s, 1H, NH); 8.35–7.95 (m, 9H, C–H, Ar); 5.23 (d, 2H,  $J = 5.2$  Hz); 5.06 (s, 1H, CH); 2.07 (s, 3H, CH<sub>3</sub>); 1.85 (s, 3H, CH<sub>3</sub>) ppm; <sup>13</sup>C NMR (100 MHz, DMSO-*d*<sub>6</sub>):  $\delta$  192.96, 163.60, 145.28, 131.71–122.84 (15 C, Ar), 95.30, 44.25, 28.44, 18.74 ppm; IR (cm<sup>-1</sup>): 3281 (N–H stretch, amine), 2862 and 2940 (C–H), 1668 (C=O), 1593 (C=C), 1187 (C–N stretch), 844 (C–H “oop”); Anal. Calcd. for C<sub>22</sub>H<sub>19</sub>NOPdCl<sub>2</sub> (490.72): C, 53.85; H, 3.90; N, 2.85. Found: C, 53.98; H, 3.98; N, 2.98%.

**Synthesis of 4.** To a solution of pyrene-tagged Pd complex **3** (10 mg, 0.02 mmol) in CH<sub>2</sub>Cl<sub>2</sub>, reduced graphene oxide (50 mg) was added. The mixture of reagents was sonicated for 10 min and then stirred for 10 h at room temperature.

The solvent was removed by using a glass filter, and the resulting catalyst was washed with sufficient amount of  $\text{CH}_2\text{Cl}_2$  and dried under vacuum at  $80^\circ\text{C}$  to give the desired rGO-supported Pd complex (**4**). The loading amount of Pd content (0.21 mmol/g) onto the graphene was measured by weight gain and ICP analyses.

**General Procedure for the Suzuki–Miyaura Coupling Reaction.** To a 10-mL reaction vial, heteroaryl halide (1.0 mmol), boronic acid (1.2 mmol),  $\text{K}_3\text{PO}_4$  (2.0 mmol), *tetra*-butylammonium bromide (TBAB) (0.5 mmol), and **4** (0.1 mol %) in water (3.5 mL) were added. The reaction mixture was stirred at  $85^\circ\text{C}$  and the reaction progress was monitored by GC–MS analysis. After completion of the reaction, it was diluted with  $\text{H}_2\text{O}$  and  $\text{CH}_2\text{Cl}_2$ . The organic layer was separated from mixture, the dried organic layer over  $\text{MgSO}_4$ , and evaporated under reduced pressure. The crude reaction product was purified using column chromatography on silica-gel to afford the corresponding product with isolated yield up to 98%.

**Procedure for Recycling the Pd Complex 4.** In the recycling experiment of the substrate, the reaction was performed according to the general procedure of the SMC reaction. After completion and cooling down of the reaction, the Pd complex **4** was separated from the mixture by centrifugation. The separated Pd complex **4** was washed with  $\text{CH}_2\text{Cl}_2$  and water and directly used for the next reaction without any change in reaction conditions.

## Results and Discussion

The (pyren-1-yl)methanamine **1** was prepared from commercially available 1-pyrenemethylamine hydrochloride under basic condition at room temperature in  $\text{CH}_2\text{Cl}_2/\text{H}_2\text{O}$ . Compound **2** was prepared by the reaction of **1** with pentane-2,4-dione in refluxing ethanol. The Pd complex **3** was prepared from **2** with  $(\text{CH}_3\text{CN})_2\text{PdCl}_2$  in acetone at  $45^\circ\text{C}$  for 2 h. The Pd complex **3** is a nonplanar and pale yellow crystalline powder, which is confirmed by density functional theory optimization and XRD analysis (Figures S1 and S2, Supporting Information). The Pd complex **4** was obtained by immersing **3** and commercially available rGO in  $\text{CH}_2\text{Cl}_2$  followed by filtration and washing repeated with an excess amount of  $\text{CH}_2\text{Cl}_2$  at room temperature (Scheme 1). The maximum loading of palladium in **4** was measured by ICP analysis (0.21 mmol/g), which exactly matched with the calculated value. The palladium complex **3** was anchored onto the rGO layer through non-covalent interaction,<sup>18,19</sup> and the presence of **3** on the rGO layers was examined by FT-IR, FE-TEM, HR-SEM, XPS, EDS, TGA, ICP, UV–vis, and Raman spectroscopy analyses. The FT-IR spectra of both complexes **3** and **4** show intense bands in the region  $1681\text{--}1644\text{ cm}^{-1}$  (Figure S3) due to the existence of carboxylato and phenyl ring stretching vibrations.<sup>20</sup> The N–H stretching peaks at  $3300\text{--}3350\text{ cm}^{-1}$  indicate the presence of the NH group.<sup>21</sup> We found an intense and broad band at  $3400\text{--}3600\text{ cm}^{-1}$

corresponding to hydroxyl group<sup>22</sup> because water molecules are usually adsorbed on the surface of rGO flakes or are inserted between the layers during sonication.<sup>23</sup> The UV–vis absorption spectrum of **4**, **3**, and rGO were analyzed (Figure 1(a)). No UV signal was found for the pure rGO sample, whereas UV signals were well overlaid for **3** and **4** due to the presence of pyrene units that absorb at 342 nm, and it proves that pyrene is grafted on the graphitic surface.<sup>24</sup> Moreover, EDS spectra showed the existence of palladium on the rGO surface (Figure 1(b)). Thus, we confirmed that the complex **3** was successfully anchored onto the graphitic surface. The morphology of **4** was observed by FE-TEM and HR-SEM analyses (Figure 1). In Figure 1(c) and (d), the TEM images of fresh **4** and that after conjugative recycling of **4** are shown. The elemental mapping by EDS performed by means of HR-SEM of catalyst **4** showed the homogeneous distribution of Pd in the hybrid materials (Figure 1(f)).

Raman spectroscopy was used to prove the structural feature of graphene-based materials. Figure 2(a) illustrates the featured areas of the Raman spectra for rGO and **4**. The  $I(\text{D})/I(\text{G})$  value in fresh rGO is 1.35, but this value in **4** decreased to 1.32, which indicated the incorporation of **3** on the graphitic surface. Moreover, an additional peak at  $432\text{ cm}^{-1}$  was observed that clearly indicated the presence of palladium on the graphitic surface,<sup>25</sup> which also confirmed by XPS survey analysis (Figure 2(c)). The thermal stability of the prepared catalyst **4** was measured using TGA analysis (Figure 2(b)).

The TGA result revealed the excellent thermal stability of **4**. It is assumed that the higher weight loss of **4** was due to the thermal decomposition of complex **3** that was anchored to the graphitic surface.

To gain further insights on the surface changes of rGO associated with the chemical reaction shown in Scheme 1, we also performed XPS analysis (Figure 3). The N 1s spectrum of **4** can be deconvoluted into three components at 399.17, 400.04, and 400.89 eV, corresponding to C–NH, N–H, and  $\text{NH}_3^+$ , respectively (Figure 3(a)).<sup>26,27</sup> The peak for C–N (285.4 eV) in **4** confirmed the presence of amino groups (Figure 3(b)). Furthermore, the O 1s spectra were reasonably fitted into a couple of peaks at 531.76 eV for C–O, and 535.57 eV for O–C=O, indicating the presence of the carbonyl group in **4** (Figure 3(c)). For the as-prepared **4**, the presence of the Pd  $3d_{3/2}$  (343.13 eV) and Pd  $3d_{5/2}$  (337.60 eV) peaks indicates the successful incorporation of Pd(II) on the graphitic surface (Figure 3(d)).<sup>28</sup>

The SMC reaction is widely used for building units of biaryl in organic synthesis,<sup>29,30</sup> and the use of inexpensive heteroaryl halides would be extremely desirable for industrial applications. Because of high stability of the catalyst **4**, efforts were immediately expanded to use this complex for the SMC of heteroaryl halides. To obtain the optimal reaction conditions, the SMC reaction of 2-bromopyridine with phenylboronic acid was performed in water using catalyst **4**, and the results are summarized in Table 1. The

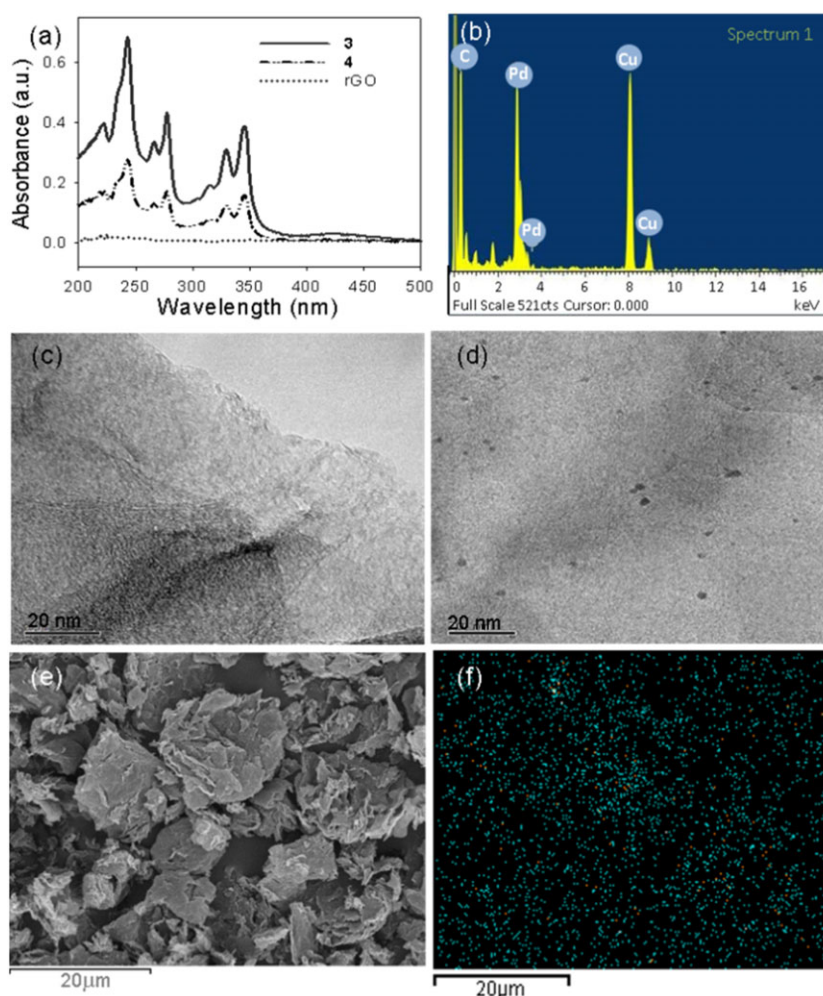


**Figure 1.** (a) UV-vis diffuse reflectance spectra of **3**, **4**, and rGO. (b) EDS analysis of **4** (note that the Cu peaks come from the copper grid). TEM images of **4** (c) before use and (d) after the fourth run. (e) SEM image of **4**. (f) EDS mapping image of catalyst **4** showing the homogeneous distribution of palladium.

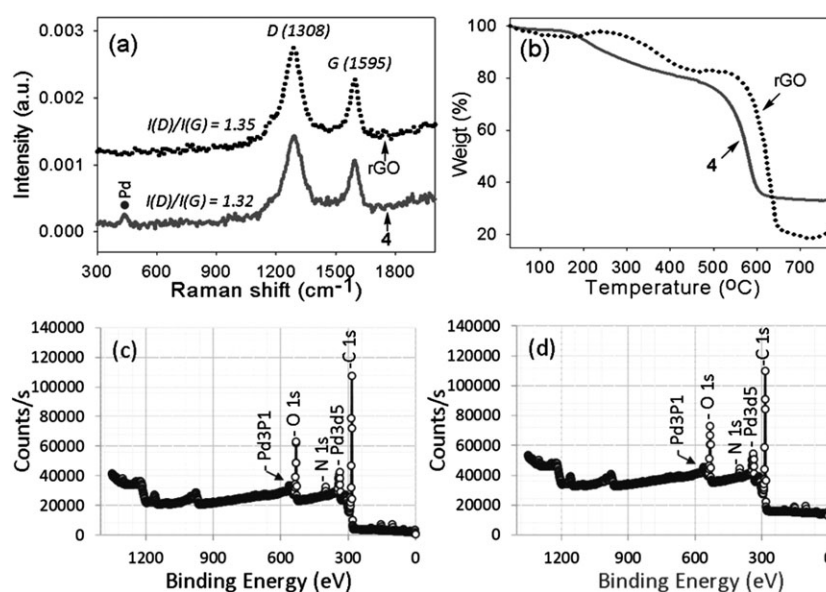


**Figure 2.** (a) Raman spectra of rGO and **4**. The corresponding  $I(D)/I(G)$  values are shown for each spectrum. (b) TGA plots of rGO and **4** with at the heating rate of  $20^{\circ}\text{C}/\text{min}$  under air. XPS analysis of catalyst **4**: (c) survey spectra and (d) survey spectra after the fourth run.

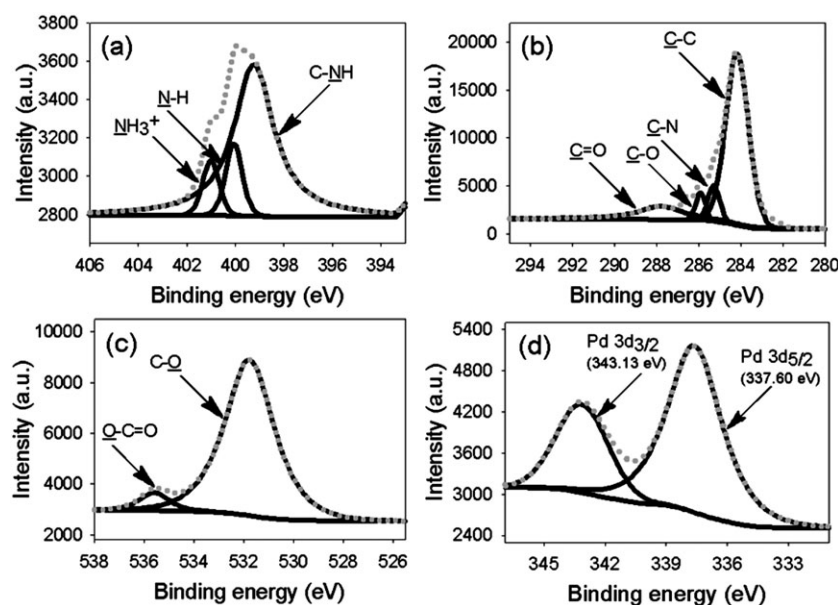
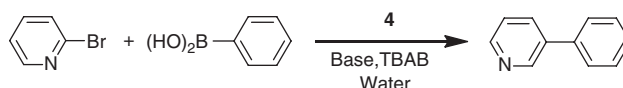


Figure 3. XPS analysis of **4**: (a) N 1s, (b) C 1s, (c) O 1s, and (d) Pd 3d.

Table 1. Optimization of **4** in the SMC reaction.<sup>a</sup>



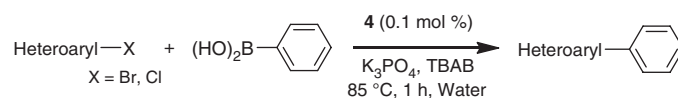
Entry	<b>4</b> (mol%)	TBAB (mmol)	Base	Time (h)	<i>T</i> (°C)	Yield <sup>b</sup> (%)
1	0.1	0	K <sub>3</sub> PO <sub>4</sub>	5	90	96
2	0.1	0.1	K <sub>3</sub> PO <sub>4</sub>	2	85	97
3	0.1	0.3	K <sub>3</sub> PO <sub>4</sub>	1.6	85	95
4	0.1	0.5	K <sub>3</sub> PO <sub>4</sub>	1	85	98
5	0.02	0.5	K <sub>3</sub> PO <sub>4</sub>	1.3	85	95
6	0.01	0.5	K <sub>3</sub> PO <sub>4</sub>	1.5	85	96
7	0.005	0.5	K <sub>3</sub> PO <sub>4</sub>	2	85	95
8	0.1	0.5	K <sub>3</sub> PO <sub>4</sub>	3	55	96
9	0.1	0.5	K <sub>2</sub> CO <sub>3</sub>	1	85	85
10	0.1	0.5	Na <sub>2</sub> CO <sub>3</sub>	1	85	83
11	0.1	0.5	CsF	1	85	76
12	0.1	0.5	KOAc	1	85	46
13	0.1	0.5	NaOH	1	85	25
14	0.1	0.5	Et <sub>3</sub> N	1	85	81
15	0.1	0.5	( <i>i</i> -Pr) <sub>2</sub> NEt	1	85	63
16	0.1	0.5	Piperazine	1	85	51
17	0.1	0.5	Et <sub>2</sub> NH	1	95	Trace
18	0.1	0.5	( <i>n</i> -Bu) <sub>3</sub> N	1	95	Trace
19	0.1	0.5	Pyridine	1	95	–

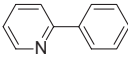
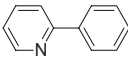
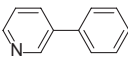
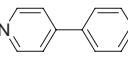
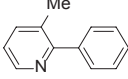
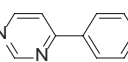
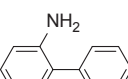
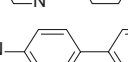
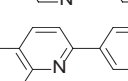
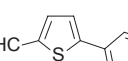
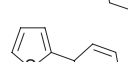
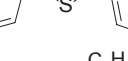
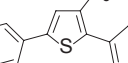
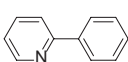
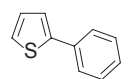
<sup>a</sup> Reaction conditions: 2-bromopyridine (1.0 mmol), PhB(OH)<sub>2</sub> (1.2 mmol), base (2.0 mmol), and water (3.5 mL).

<sup>b</sup> Isolated yield is given in parenthesis.

yield of the products gradually increased with increase of the loading amount of **4** (0.005–0.1 mol %). Furthermore, to get higher efficiency of **4**, we have changed the amounts of TBAB as an additive and base. The initial reaction was performed without TBAB using 0.1 mol %

of **4** and K<sub>3</sub>PO<sub>4</sub> as base in water at 90°C to give the corresponding coupling product in 97% yield within 5 h (entry 1). Then, the phase-transfer additive TBAB was added in the reaction mixture to enhance the reaction yield. As expected, the yield of the coupling product significantly

**Table 2.** SMC of heteroaryl halides in water.<sup>a</sup>

Entry	Aryl halide	Product	Yield <sup>b</sup> (%)
1 <sup>c</sup>			0
2			100 (98)
3			97 (95)
4			98 (96)
5			83 (81)
6			96 (94)
7			85 (82)
8			91 (88)
9			81 (80)
10			100 (98)
11			100 (98)
12 <sup>d</sup>			99 (97)
13 <sup>d</sup>			86 (84)
14 <sup>e</sup>			100 (96)
15 <sup>e</sup>			95 (93)
16 <sup>e</sup>			90 (88)

<sup>a</sup> Reaction conditions: heteroarylhalide (1.0 mmol), PhB(OH)<sub>2</sub> (1.2 mmol), K<sub>3</sub>PO<sub>4</sub> (2.0 mmol), TBAB (0.5 mmol) and water (3.5 mL).

<sup>b</sup> GC yields; isolated yield is given in parenthesis.

<sup>c</sup> rGO used as catalyst.

<sup>d</sup> PhB(OH)<sub>2</sub> (2.4 mmol), K<sub>2</sub>CO<sub>3</sub> (3.0 mmol) and **4** (0.2 mol%).

<sup>e</sup> 90°C for 6 h.

increased with a simultaneous decrease of the reaction time and temperature when 0.1–0.5 mmol of TBAB was added (entries 2–4). It was observed that high catalytic activity still maintained at a very small (0.01–0.005 mol %) amount of catalyst loading (entries 5–7). It is also noteworthy that **4** efficiently promoted this coupling reaction even at 55°C to provide the corresponding product in 96% yield within 3 h (entry 8).

Among the various bases screened in water, the relatively weak and less expensive  $K_3PO_4$  gave the best result (entry 4), while many other inorganic bases showed only moderate activities (entries 9–13). Organic bases showed lower activities than the inorganic bases used (entries 14–19). After successful screening of the cross-coupling reaction, we carried out SMC reaction of several less reactive heteroaryl halides, and control experiment using rGO under very similar conditions were applied, showing that the Pd-free material was completely ineffective (Table 2, entry 1). Outstanding catalytic efficiency was observed for the coupling reactions of various *N*-heteroaryl bromides with boronic acid at 85°C to give the corresponding coupling products in excellent yields (entries 2–9). It is therefore remarkable that catalyst **4** successfully induced the SMC reactions of heteroaryl halides as well as heteroaryl amino bromides. Further extension to the coupling of heteroarylthiophenes with boronic acid also provided the desired products in high yields (entries 10–13). Even successful couplings of the less reactive 2,5-dibromothiophene and 2,5-dibromo-3-hexylthiophene with both steric hindrance and strong electron-donating hexyl side chain with boronic acid were observed (entries 12, 13). It should be noted that **4** efficiently promoted the SMC reaction of heteroaryl chlorides to afford the corresponding products in high yield (entries 14–16). Moreover, catalyst **4** showed high efficiency toward aryl chlorides but with a slightly longer reaction time and higher temperature. This could be attributed to the different bond strengths of C–Br and C–Cl with different electron-withdrawing powers of the halogen substituents.<sup>31</sup>

Further, we turned our attention to catalyst reusability under mild condition. The recycling of **4** was investigated in the coupling of 2-bromopyridine with phenylboronic acid (Figure 4). Catalyst **4** showed high catalytic activity (100–98% conversion) and could be recycled more than five times without significant loss of catalytic activity. The possible leaching of Pd after completion of the reaction was monitored by ICP-MS, proving a total loss of 0.9 wt %. Comparative TEM studies of catalyst **4** before and after the experiments are shown in Figure 1. When used catalyst was compared with the fresh one, Pd nanoparticles dispersed on the rGO could be seen after several runs of the reaction. The result of this study was in agreement with those in the literature that the formation of Pd nanoparticles on the rGO surface as an active species developed during reaction.<sup>14,32</sup> The extremely high stability and reusability of the prepared catalyst could be attributed to the strong non-covalent interaction between the pyrene moiety and the graphitic surface. The FT-IR and XPS survey spectra of used

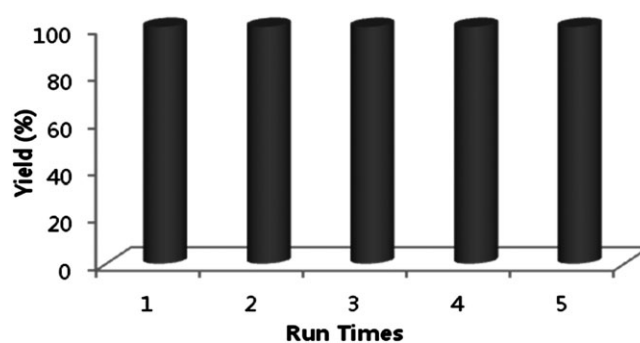


**Figure 4.** Recycling experiment for coupling 2-bromopyridine using **4**. The reaction conditions are the same as in Table 1 (entry 2).

**4** were indistinguishable from those of the fresh catalyst **4** (Figures 2(c), (d), and S3), suggesting that no structural variation or deformation of the catalyst occurred during the reaction under the defined conditions.

## Conclusion

In conclusion, we have designed and developed a highly active nanoparticle-supported heterogeneous palladium catalyst for coupling reactions in water. The catalyst demonstrated that a wide range of less reactive heteroaryl halides could be successfully coupled under mild reaction conditions. In particular, the activity of the catalyst was fully maintained during reuse. We strongly believe that this heterogeneous catalytic system, in combination with its efficiency in coupling reactions of less reactive heteroaryl substrates, may inspire future research in the field of organic synthesis and catalytic engineering.

**Acknowledgment.** This work is supported by an Inha University Research Grant (2014).

**Supporting Information.** Additional supporting information is available in the online version of this article.

## References

1. D. Zhao, J. You, C. Hu, *Chem. Eur. J.* **2011**, *17*, 5466.
2. R. Martin, S. L. Buchwald, *Acc. Chem. Res.* **2008**, *41*, 1461.
3. S. Santra, P. K. Hota, R. Bhattacharyya, P. Bera, P. Ghosh, S. K. Mandal, *ACS Catal.* **2013**, *3*, 2776.
4. T. Noel, S. Kuhn, A. J. Musacchio, K. F. Jensen, S. L. Buchwald, *Angew. Chem. Int. Ed.* **2011**, *50*, 5943.
5. T. Kinzel, Y. Zhang, S. L. Buchwald, *J. Am. Chem. Soc.* **2010**, *132*, 14073.
6. J. M. Fraile, J. I. Garcia, J. A. Mayoral, *Chem. Rev.* **2009**, *109*, 360.
7. D. J. Cole-Hamilton, *Science* **2003**, *299*, 1702.
8. W. A. Herrmann, C. W. Kohlpaintner, *Angew. Chem.* **1993**, *105*, 1588.
9. A. Taher, J.-B. Kim, J.-Y. Jung, W.-S. Ahn, M.-J. Jin, *Synlett* **2009**, *15*, 2477.

10. J. Horniakova, T. Raja, Y. Kubota, Y. Sugi, *J. Mol. Catal. A* **2004**, *217*, 73.
11. Y. Uozumi, *Bull. Chem. Soc. Jpn.* **2008**, *81*, 1183.
12. R. Andrs, E. de Jesffls, J. C. Flores, *New J. Chem.* **2007**, *31*, 1161.
13. A. Garcia-Bernab, C. C. Tzschucke, W. Bannwarth, R. Haag, *Adv. Synth. Catal.* **2005**, *347*, 1389.
14. S. Sabater, J. A. Mata, E. Peris, *ACS Catal.* **2014**, *4*, 2038.
15. L. Rodriguez-Perez, M. A. Herranz, N. Martin, *Chem. Commun.* **2013**, *49*, 3721.
16. A. Le Goff, B. Reuillard, S. Cosnier, *Langmuir* **2013**, *29*, 8736.
17. M. Keller, V. Colliere, O. Reiser, A.-M. Caminade, J.-P. Majoral, A. Ouali, *Angew. Chem. Int. Ed.* **2013**, *52*, 3626.
18. F. J. Gomez, R. J. Chen, D. Wang, R. M. Waymouth, H. Dai, *Chem. Commun.* **2003**, 190.
19. G. L. Liu, B. Wu, J. Zhang, X. Wang, M. Shao, J. Wang, *Inorg. Chem.* **2009**, *482*, 383.
20. S. Bhattacharjee, D. A. Yang, W. S. Ahn, *Chem. Commun.* **2011**, *47*, 3637.
21. S. N. Kim, S. T. Yang, J. Kim, J. E. Park, W. S. Ahn, *CrytEngComm* **2012**, *14*, 4142.
22. Y. Nie, T. Hubert, *Polym. Int.* **2011**, *60*, 1574.
23. X. Zhang, S. Wan, J. Pu, L. Wang, X. Liu, *J. Mater. Chem.* **2011**, *21*, 12251.
24. Y. Shiraishi, Y. Tokitoh, T. Hirai, *Org. Lett.* **2006**, *8*, 3841.
25. V. B. Parambath, R. Nagar, K. Sethupathi, S. Ramaprabhu, *J. Phys. Chem. C* **2011**, *115*, 15679.
26. D. Yang, A. Velamakanni, G. Bozoklu, S. Park, M. Stoller, R. D. Piner, S. Stankovich, I. Jung, D. A. Field, C. A. V. Jr, R. S. Ruoff, *Carbon* **2009**, *47*, 145.
27. M. Wang, Y. Zhao, R. Xu, M. Zhang, R. K. Y. Fu, P. K. Chu, *Diamond Relat. Mater.* **2013**, *38*, 28.
28. N. Brun, P. Hesemann, G. Laurent, C. Sanchez, M. Birot, H. Deleuze, R. Backov, *New J. Chem.* **2013**, *37*, 157.
29. G. A. Molander, B. Canturk, *Angew. Chem. Int. Ed.* **2009**, *48*, 9240.
30. B. Milde, D. Schaarschmidt, T. Ruffer, H. Lang, *Dalton Trans.* **2012**, *41*, 5377.
31. F. Alonso, I. P. Beletskaya, M. Yus, *Tetrahedron* **2008**, *64*, 3047.
32. S. K. Movahed, R. Esmatpoursalmani, A. Bazgir, *RSC Adv.* **2014**, *4*, 14586.